

# A Comparative Analysis of the Fibulin Protein Family

## BIOCHEMICAL CHARACTERIZATION, BINDING INTERACTIONS, AND TISSUE LOCALIZATION\*

Received for publication, November 30, 2006, and in revised form, February 6, 2007. Published, JBC Papers in Press, February 26, 2007, DOI 10.1074/jbc.M611029200

Naoyuki Kobayashi<sup>‡</sup>, Günter Kostka<sup>†1</sup>, Jörg H. O. Garbe<sup>‡</sup>, Douglas R. Keene<sup>§</sup>, Hans Peter Bächinger<sup>§¶1</sup>, Franz-Georg Hanisch<sup>||</sup>, Dessislava Markova<sup>\*\*</sup>, Takeshi Tsuda<sup>††</sup>, Rupert Timpl<sup>‡2</sup>, Mon-Li Chu<sup>\*\*</sup>, and Takako Sasaki<sup>‡3</sup>

From the <sup>‡</sup>Max-Planck-Institut für Biochemie, D-82152 Martinsried, Germany, the <sup>§</sup>Shriners Hospital for Children and the <sup>¶</sup>Department of Biochemistry and Molecular Biology, Oregon Health and Science University, Portland, Oregon 97239, the <sup>||</sup>Institute for Biochemistry II, Medical Faculty, and Center for Molecular Medicine Cologne (CMMC), University of Cologne, D-50931 Cologne, Germany, the <sup>\*\*</sup>Department of Dermatology and Cutaneous Biology, Thomas Jefferson University, Philadelphia, Pennsylvania 19107, and <sup>††</sup>Nemours Cardiac Center and Nemours Biomedical Research, Alfred I. DuPont Hospital for Children, Wilmington, Delaware 19899

Fibulins are a family of five extracellular matrix proteins characterized by tandem arrays of epidermal growth factor-like domains and a C-terminal fibulin-type module. They are widely distributed and often associated with vasculature and elastic tissues. In this study, we expressed the three more recently identified family members, fibulin-3, fibulin-4, and fibulin-5, as recombinant proteins in mammalian cells. The purified proteins showed short rod structures of ~20 nm with a globule at one end, after rotary shadowing and electron microscopy. Two forms of mouse fibulin-3 were purified, and the O-glycan profiles of the larger form were characterized. Polyclonal antibodies raised against the purified proteins did not show any cross-reactivity with other family members and were used to assess the levels and localization of the fibulins in mouse tissues. Their binding interactions, cell adhesive properties, and tissue localization were analyzed in parallel with the previously characterized fibulin-1 and -2. Binding to tropoelastin was strong for fibulin-2 and -5, moderate for fibulin-4 and -1, and relatively weak for fibulin-3. Fibulin-4, but not fibulin-3 and -5, exhibited distinct interactions with collagen IV and nidogen-2 and moderate binding to the endostatin domain from collagen XV. Cell adhesive activities were not observed for all fibulins, except mouse fibulin-2, with various cell lines tested. All five fibulins were found in perichondrium and various regions of the lungs. Immunoelectron microscopy localized fibulin-4 and -5 to fibrillin microfibrils at distinct locations. Our studies suggest there are unique and redundant functions shared by these structurally related proteins.

Fibulins are a family of extracellular glycoproteins with distinctive features of a fibulin-type C-terminal domain preceded by tandem calcium-binding (cb)<sup>4</sup> epidermal growth factor (EGF)-like modules (1–3). The five-member family can be further classified into two subgroups. Fibulin-1 and -2, the first subgroup, are substantially larger than the other three members of the family because of the presence of an extra domain with three anaphylatoxin modules and higher numbers of cbEGF modules (see Fig. 1). Fibulin-1 at 90–100 kDa has variable C-terminal domains. Two major splice variants, fibulin-1C and -1D, are present in approximately equal amounts in most tissues of all animal species studied to date. Fibulin-2 at 200 kDa is the largest of all the fibulins, because it possesses an additional N-terminal domain of ~400 amino acids not found in other fibulins. Members of the second subgroup, fibulin-3, -4, and -5, are similarly small in size (50–60 kDa) and highly homologous to one another in modular structure. They consist of a modified cbEGF domain at the N terminus followed by five tandem cbEGF modules and the fibulin-type C-terminal region (Fig. 1).

Fibulin-1 and -2, the first subgroup, have been characterized extensively and shown to display distinct yet overlapping molecular interactions and expression patterns. Both proteins are localized in basement membranes, elastic fibers, and other connective tissue structures (4–7). Fibulin-1 also is a plasma protein (8, 9), and its expression can be detected very early during embryonic development in most basement membranes (10). Fibulin-2 expression initiates later during embryonic development and is distributed in a more restricted manner compared with fibulin-1. Notably, these two fibulins are both prominently expressed in the endocardial cushion tissue, great vessels, and developing cartilages during embryogenesis and remain abundant in the cardiac valves and blood vessel walls in the postnatal stage (7, 10–12). They both are able to bind fibronectin, proteoglycans, tropoelastin, and various elastic

\* This work was supported by the Deutsche Forschungsgemeinschaft (DFG) (Grants Sa 1003/1 and -2), the European Commission (Grant QLK3-CT2000-00084 to R. T. and T. S.), the DFG (Grants Ha 2092/11-1 and -2 to F. G. H.), Shriners Hospital for Children (to H. P. B. and D. R. K.), and National Institutes of Health Grant GM55625 (to M. L. C.). The costs of publication of this article were defrayed in part by the payment of page charges. This article must therefore be hereby marked "advertisement" in accordance with 18 U.S.C. Section 1734 solely to indicate this fact.

<sup>1</sup> Deceased on January 19, 2006.

<sup>2</sup> Deceased on October 20, 2003.

<sup>3</sup> To whom correspondence should be addressed: The Shriners Hospital for Children, 3101 SW Sam Jackson Park Rd., Portland, OR 97239. Tel.: 503-221-3782; Fax: 503-221-3451; E-mail: txs@shcc.org.

<sup>4</sup> The abbreviations used are: cb, calcium binding; EGF, epidermal growth factor; NEM, N-ethylmaleimide; TBS, Tris-buffered saline; PMSF, phenylmethylsulfonyl fluoride; ESI-MS, electrospray ionization-mass spectrometry; MALDI, matrix-assisted laser desorption/ionization; TIMP, tissue inhibitor of metalloproteinase; E, embryonic day.

## A Comparative Analysis of the Fibulin Protein Family

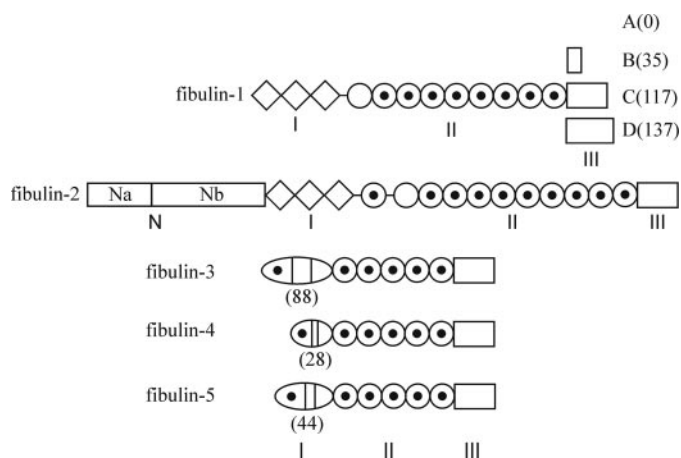


**FIGURE 1. The modular domain structure of fibulins.** The fibulins are characterized by a tandem array of EGF-like repeats (domain II) and the fibulin-type C-terminal module (domain III). The EGF-like modules are represented as circles, and those with a dot possess a consensus motif for calcium binding (cb). Diamonds in domain I of fibulin-1 and -2 indicate anaphylatoxin-like modules. Domain N, which is unique to fibulin-2, can be subdivided into a Cys-rich segment (*Na*) and a Cys-free segment (*Nb*). Fibulin-3, -4, and -5 have a modified cbEGF-like module at their N terminus. This modified cbEGF-like module has an extra Cys<sup>5</sup>-Cys<sup>6</sup> loop at the beginning of the module and a long linker region between Cys<sup>2</sup>-Cys<sup>4</sup> and Cys<sup>5</sup>-Cys<sup>6</sup> loops. The residues between Cys<sup>4</sup> and Cys<sup>5</sup> are shown in parentheses. Four different alternative splice variants are reported for human fibulin-1, shown as variants A–D, and the numbers in parentheses indicate residues of domain III. Mice and presumably most other species express only variants C and D.

fiber and basement membrane proteins (2), thereby participating in diverse extracellular supramolecular structures.

The three smaller fibulins have been named using various acronyms before were classified as a family. Fibulin-3 is also known as S1–5 and EFEMP1, fibulin-4 as MBP1 and EFEMP2, and fibulin-5 as EVEC and DANCE. Fibulin-3 was initially identified as a gene highly up-regulated in senescent and Werner syndrome fibroblasts (13). Genetic linkage and molecular analysis has associated a missense mutation (R345W) in fibulin-3 with heritable macular degenerative disorders, and the protein has been shown to be localized in Bruch's membrane of the retina (14, 15). Fibulin-4 was identified through its sequence homology to fibulins-1, -2, and -3 and independently as a protein interacting with a mutant form of the tumor suppressor protein p53 (16, 17). The interaction with an intracellular protein may be explained by the presence of an alternative fibulin-4 transcript lacking the signal peptide coding sequences (18). Fibulin-5 was first characterized as a gene strongly expressed in large blood vessels during embryonic development and highly up-regulated upon vascular injury (19, 20). Through targeted ablation of genes in mice, both fibulin-4 and -5 have been shown to play essential roles in the assembly of elastic fibers during development, and both proteins bind tropoelastin *in vitro* (21–23). Mutations in fibulin-4 and -5 in humans lead to the cutis laxa syndrome, characterized by loose skin, emphysematous lungs, and tortuous blood vessels resulting from paucity and fragmentation of elastic fibers (24–26). Additionally, amino acid substitutions in fibulin-5 have been implicated in age-related macular degeneration (27).

Despite the involvement of the three fibulins of the second subgroup in human diseases, relatively little is known about their biochemical properties, molecular interactions, and

expression patterns. In this study, we have prepared recombinant fibulin-3, -4, and -5 in their native forms without peptide tags in mammalian cells and raised specific antibodies. We performed a comprehensive biochemical analysis of these three fibulins in parallel with the previously characterized first subgroup. Our studies show that members of the fibulin protein family have unique and partially overlapping binding interactions and expression patterns, suggesting that they serve both distinct and redundant functions.

## EXPERIMENTAL PROCEDURES

**Sources of Proteins**—Laminin-1, collagen IV, and perlecan were purified from the mouse Engelbreth-Holm-Swarm tumor (28). Mouse nidogen-1 (29), mouse nidogen-2 (30), mouse fibulin-1 (31), and mouse fibulin-2 (4) and endostatins derived from collagens XV and XVIII (32) were obtained as recombinant products as described previously. Human plasma fibronectin (Behringwerke) and vitronectin were purified by chromatography on heparin-Sepharose (33). Recombinant human tropoelastin was kindly provided by Dr. Joel Rosenbloom (University of Pennsylvania). Integrin  $\alpha$ V $\beta$ 3 was purified by affinity chromatography from human placenta (34).

**Expression Vectors and Recombinant Protein Production**—To obtain a full-length cDNA encoding mouse fibulin-3, total RNA isolated from mouse lungs was amplified by reverse transcription-PCR using primers 5'-GTCAGCTAGCAGAGAAT-CACGATGTTG (forward) and 5'-GTCAGCTCGAGCTAAAA-TGAAAATGGCCCC (reverse). IMAGE cDNA clones for mouse fibulin-4 (3980048), mouse fibulin-5 (3482574), and human fibulin-5 (4693953) were used as templates to PCR amplify the full-length cDNAs. The primers for mouse fibulin-4 were 5'-GTCA-GCTAGCCTCAGGATGCTCCC (forward) and 5'-GTCAGCTC-GAGTCAGAAGGTATAGGCTCCC (reverse), and for mouse fibulin-5 were 5'-GTCAGCTAGCGCATCTTGGATATGC-CAGG (forward) and 5'-GCCACTCGAGTCAGAACGGAT-ACTGCGAC (reverse). The 5' primers contained an NheI site, and the 3' primers had an XhoI site following the stop codons. The resulting full-length cDNAs were inserted into the NheI and XhoI sites of the episomal expression vector pCEP-Pu (35). For human fibulin-5, the cDNA was amplified using primers 5'-GTCAGCTAGCACAGGCACAGTGCACG (forward) and 5'-GTCAGCTCGAGTCAGAATGGGTACTGCGAC (reverse), and the cDNA fragment flanked by NheI and XhoI sites was inserted into a pCEP-Pu expression vector containing the BM-40 signal peptide (35). Mouse MAGP-1 and MAGP-2 were also prepared recombinantly. IMAGE cDNA clones for MAGP-1 (6516202) and MAGP-2 (5325744) were used as templates, and the 5' primers contained an NheI site and the 3' primers contained an XhoI site for cloning into pCEP-Pu vector as described above. The sequences of all PCR products were confirmed by cycle sequencing using a BigDye Terminator Cycle Sequencing Ready Kit (ABI). These expression constructs were transfected into human embryonic kidney 293-EBNA cells, and serum-free media were collected as described (35).

**Purification and Characterization of Recombinant Proteins**—For purification of mouse fibulin-3, mouse fibulin-5, and human fibulin-5, conditioned media were passed over a DEAE-cellulose column equilibrated in 0.05 M Tris-HCl, pH 8.6, and eluted

with a linear 0–0.5 M NaCl gradient. Mouse fibulin-3 was eluted at 0.2–0.3 M NaCl, whereas mouse and human fibulin-5 eluted at 0.25–0.35 M NaCl. They were next purified on a Superose 12 column (HR16/50) equilibrated in 0.3 M NaCl/0.05 M Tris-HCl, pH 8.0, and then on a Mono Q (HR5/5) column equilibrated in 2 M urea/0.02 M Tris-HCl, pH 8.0. Two different forms of fibulin-3 were purified, and they were eluted at 0.2–0.23 M NaCl and 0.23–0.3 M NaCl from the Mono Q column. Both mouse and human fibulin-5 were eluted at 0.3–0.35 M NaCl from the Mono Q column. The purification of mouse fibulin-4 followed the same protocol except that the DEAE-cellulose, and Superose 12 columns were run in the presence of 2 M urea. Fibulin-4 was eluted at 0.3–0.34 M NaCl from the Mono Q column. All purified proteins were dialyzed against 0.2 M ammonium bicarbonate.

Purification of MAGP-1 and MAGP-2 were performed basically by the same method as described above for the fibulins. From DEAE-cellulose, MAGP-1 was eluted at 0.3–0.4 M NaCl and MAGP-2 at 0.2–0.3 M NaCl. For the Superose 12 column, the buffers used were either 0.3 M NaCl/0.05 M Tris-HCl, pH 8.0, or 2 M urea/0.05 M Tris-HCl, pH 8.0. Both proteins were eluted through most of the fractions, indicating oligomerization of the proteins. The separation was not improved in the presence of 2 M urea. The monomer fractions were pooled and used for binding assays.

Protein concentrations were determined on a Biotronik LC 3000 amino acid analyzer after hydrolysis with 6 M HCl for 16 h at 110 °C. N-terminal sequencing by Edman degradation was performed on a Procise sequencer (Applied Biosystems) following the manufacturer's instructions. Briefly, fibulins were separated by SDS-PAGE under reducing conditions and blotted onto polyvinylidene difluoride membranes. The stained bands were cut out, incubated with pyroglutamate aminopeptidase (TaKaRa Bio), and then sequenced. Electron microscopy of rotary shadowed proteins was carried out using standard protocols (36).

**Laser Light Scattering and Analytical Ultracentrifugation**—The molecular weights of the recombinant fibulin-4 and -5 were determined by quasielastic laser light scattering (Dawn Eos, Wyatt Technology Corp.). The samples were chromatographed using a Superose 12 HR10/30 column equilibrated in 0.25 M NaCl/20 mM HEPES (pH 7.0), and the intensity of scattered light was simultaneously detected at 18 different angles. The absorbance and refractive index were also measured with in-line detectors. The molecular weight of the samples was then calculated using Astra software provided with the instrument. For sedimentation equilibrium, measurements were done in double sector cells on a Beckman XLA analytical ultracentrifuge. The temperature of the runs was either 4 or 20 °C, and the speed was 12,000 rpm. The concentration was monitored at 230 nm as a function of the radial distance, and the data were analyzed by non-linear least squares fitting (Scientist, Micromath, St. Louis, MO).

**Treatment with Glycosidases**—5  $\mu$ g of lyophilized fibulins was dissolved in 18  $\mu$ l of 20 mM phosphate buffer (pH 7.2) containing 1 mM EDTA, 0.5 mM *N*-ethylmaleimide (NEM) and 1 mM Pefabloc (Roche Applied Science) and incubated with neuraminidase (Roche Applied Science) and *O*-glycosidase

(Roche Applied Science) in the presence or absence of *N*-glycosidase F (Roche Applied Science) at 37 °C for 24 h. *N*-Glycosidase F treatment was also done after denaturation of proteins by heating at 95 °C for 5 min in the presence of 1% SDS and 1%  $\beta$ -mercaptoethanol.

**Reductive  $\beta$ -Elimination and Permethylation of Glycan Alditols**—For structural studies the glycans were liberated by reductive  $\beta$ -elimination according to a protocol applicable to microscale samples (37). The *O*-glycoprotein (10–30  $\mu$ g) was dried in a 0.5-ml Eppendorf vial and treated with freshly prepared 0.5 M NaBH<sub>4</sub> in 50 mM NaOH (20  $\mu$ l) overnight at 50 °C. The sample was desalted with a 50- $\mu$ l aliquot of Dowex 50Wx8(H<sup>+</sup>). To remove boric acid, 50- $\mu$ l aliquots of 1% acetic acid in methanol were added to the dry sample (5 $\times$ ) and evaporated under nitrogen at 40 °C. To the dry sample 50  $\mu$ l of anhydrous Me<sub>2</sub>SO was added followed by the same volume of base (NaOH/Me<sub>2</sub>SO), and the mixture was incubated for 30 min at room temperature with occasional shaking. Finally, an aliquot of 25  $\mu$ l of methyl iodide was pipetted to the frozen reaction mixture followed by incubation for 30 min at room temperature. After neutralization with dilute acetic acid, the methylated glycans were extracted with chloroform-water. The chloroform phase was dried under nitrogen, and the glycans were solubilized in methanol.

**Analysis of *O*-Glycans by Mass Spectrometry**—Matrix-assisted laser desorption ionization (MALDI) mass spectrometry was performed on a Bruker Reflex IV instrument (Bruker Daltonics, Bremen, Germany). The methylated glycan samples (~500 pmol per  $\mu$ l) contained in methanol were applied to the stainless steel target by mixing a 0.5- $\mu$ l aliquot with 1.0  $\mu$ l of matrix (saturated solution of 2,5-dihydroxybenzoic acid in acetonitrile/0.1% trifluoroacetic acid, 1:2). Analyses were performed by positive ion detection in the reflectron mode as described previously (38). Electrospray ionization (ESI) mass spectrometry data were acquired on a Q-ToF two-quadrupole-time of flight mass spectrometer (Waters, Eschborn, Germany) equipped with a Z spray source. Mass spectrometry was performed in the positive ion mode using previously described conditions (38). Collision energies varied in accordance with the type of molecular ion (M+Na: 50–75 V; M+H: 15–30 V).

**Site Determination of *O*-Glycosylation**—Three independent strategies were applied to identify *O*-glycosylated peptides after proteolytic digestion. A first aliquot was partially deglycosylated by successive exoglycosidase treatment with sialidase (*Clostridium perfringens*, New England Biolabs, 100 milliunits, pH 6.0, 24 h),  $\beta$ -galactosaminidase (bovine kidney, Glyco, sodium citrate, pH 6.0, 24 h), and  $\beta$ -hexosaminidase (Glyco, 100 milliunits, pH 6.0, 24 h), followed by reduction and alkylation according to standard protocols. The sample was successively digested with trypsin and V8 protease, and the peptide fragments were isolated by solid-phase extraction on a Pep-Clean C18 Spin column (Pierce). In a second approach, the protein was desialylated by mild acid treatment (0.1 M aqueous trifluoroacetic acid, 80 °C, 1 h), followed by trypsin/V8 digestion of the reduced and alkylated sample. In a third approach, the sample was reduced and alkylated prior to trypsin and V8 treatment, but the peptides and glycopep-

## A Comparative Analysis of the Fibulin Protein Family

tides were analyzed without cleavage of the sugars by ESI-q-trap mass spectrometry (see below).

MALDI-MS was performed under conditions described above. Nanoflow LC with online ESI-MS was performed on a Q-ToF2 quadrupole-time-of-flight mass spectrometer (Waters, Manchester, UK) equipped with a Z spray source. Samples were introduced using the Ultimate nano-LC system (LC-Packings, Amsterdam, Netherlands) equipped with the Famos autosampler and the Switchos column switching module. The column setup comprised a  $0.3 \times 1$ -mm trap column and a  $0.075 \times 150$ -mm analytical column, both packed with 3- $\mu$ m PepMap C18 (LC-Packings). The analytical column flow rate was  $\sim 200$  nl/min, resulting from a 1:1000 split of the 200  $\mu$ l/min flow delivered by the system pump. The samples were eluted onto the analytical column by using a gradient of acetonitrile in 0.1% formic acid over 30 min.

**Binding Assays**—Protein ligands immobilized onto plastic wells were incubated with various concentrations of soluble ligands, and binding was detected with specific antisera against the soluble ligands following methods described previously (39). The binding reactions were carried out in a buffer containing 0.15 M NaCl/0.05 M Tris-HCl (pH7.4) (TBS) supplemented with 2 mM  $\text{CaCl}_2$ . For integrin  $\alpha V\beta 3$  binding assays, wells were coated with purified integrin dissolved in TBS containing 2 mM  $\text{MgCl}_2$ , and the binding buffer used was TBS containing 1 mM  $\text{MnCl}_2$ , 1 mM  $\text{MgCl}_2$ , 0.1 mM  $\text{CaCl}_2$ , and 0.01% Tween 20.

**Cell Attachment Assays**—Adhesion of established cell lines and human umbilical cord endothelial cells to ligand-coated plastic wells was carried out for 30–60 min and detected colorimetrically according to a previously described protocol (40).

**Immunological Assays**—Immunization of rabbits, affinity purification of antibodies, enzyme-linked immunosorbent assay titration, and radioimmunoassays were carried out using established protocols (41).

Fibroblasts obtained from 14.5-day mouse embryos were cultured in Dulbecco's modified Eagle's medium supplemented with 10% fetal calf serum. Confluent cells grown on a 10-cm dish were used to obtain serum-free culture medium (5 ml), and the cell layers were extracted consecutively with three different buffers (1 ml/each) as described previously (42). These included a detergent extract with TBS containing 1% Nonidet P-40, 0.5% deoxycholate, 0.1% SDS, 2 mM phenylmethylsulfonyl fluoride (PMSF) and 0.5 mM NEM; an EDTA extract with TBS containing 10 mM EDTA, 2 mM PMSF, and 0.5 mM NEM; and a urea extract with TBS containing 6 M urea, 2 mM PMSF, and 0.5 mM NEM.

Tissues from 5- to 7-week-old mice were homogenized (200 mg of tissue/ml) in TBS containing 10 mM EDTA, 2 mM PMSF, and 0.5 mM NEM. The homogenates were centrifuged, and the supernatants were collected (EDTA extracts). The residual materials were extracted with the same buffer containing in addition 1% Nonidet P-40, 0.5% sodium deoxycholate, 0.1% SDS. The homogenates were centrifuged to collect the supernatants (detergent extracts). The precipitates were further extracted with 6 M guanidine hydrochloride/50 mM Tris-HCl (pH 7.5) at 4 °C overnight, and then centrifuged to collect the supernatant (guanidine extracts). Protein contents of the extracts were determined with BCA assay (Pierce).

Cell and tissue extracts were separated by 5–20% SDS-PAGE gels and electroblotted onto Immobilon-P membrane (Millipore, Bedford, MA) followed by incubation with antibodies. The bound antibodies were detected with ECL Western blotting reagents (Amersham Biosciences).

**Immunohistochemistry**—Mouse embryos obtained by mating of C57BL/6 mice (Jackson Laboratories) were harvested at day 15 of gestation (E15), fixed in 4% paraformaldehyde overnight, and cryosectioned at a thickness of 7–8  $\mu$ m. Frozen sagittal sections of E14 mouse embryos were obtained from Zyangen (San Diego, CA). Affinity-purified antibodies of fibulins were used at a concentration of 5  $\mu$ g/ml for immunohistochemistry. Tissue sections were incubated with primary antibodies overnight, and immunoreactivity was revealed by Cy-3-conjugated goat anti-rabbit IgG (Jackson ImmunoResearch). Microscopic examination was performed with a Zeiss Axioskop epifluorescence microscope, and images were obtained with a Toshiba 3CCD camera.

**Immunoelectron Microscopy**—Newborn mouse perichondrium was labeled using *en bloc* diffusion of primary antibodies (43) followed by secondary anti-rabbit IgG conjugated with 5 nm gold particles.

## RESULTS

**Expression and Purification of Recombinant Fibulins**—Mouse fibulin-3 and fibulin-4, and both mouse and human fibulin-5 were prepared in recombinant forms using human embryonic kidney 293 cells transfected with the expression constructs. The recombinant fibulins were secreted into culture media at a concentration of 1–2  $\mu$ g/ml except for mouse fibulin-4, which was produced at 5–10  $\mu$ g/ml. All fibulins could be purified by similar chromatographic steps as described under “Experimental Procedures.” They appeared homogenous by SDS-gel electrophoresis (Fig. 2A) and by N-terminal amino acid sequencing. The molecular masses determined by SDS-PAGE under reducing conditions were 80 and 63 kDa for mouse fibulin-3 (see below), 61 kDa for mouse fibulin-4, 66 kDa for mouse fibulin-5, and 64 kDa for human fibulin-5 (Fig. 2A). A distinct increase in electrophoretic mobility for all fibulins was observed under non-reducing conditions (data not shown), suggesting the existence of many intramolecular disulfide bonds. The N-terminal sequences of the recombinant mouse fibulin-3, -4, and -5 were found to be blocked, suggesting that the predicted glutamine residues at the N termini of these proteins are cyclized. This possibility was verified by pyroglutamate aminopeptidase treatment prior to Edman degradation, which yielded YTEEI for fibulin-3 and DTEEPDS for fibulin-4 as predicted from the primary sequences. However, the enzyme treatment failed to generate any amino acid sequence for mouse fibulin-5 with the predicted N-terminal sequence of QQQCTN. Human fibulin-5 was expressed using the vector containing the BM-40 signal peptide, which introduced a novel N-terminal APLA sequence after processing (44). Edman degradation of the recombinant human fibulin-5 gave the expected N-terminal sequence of APLAQAQ.

Two forms of mouse fibulin-3 that differ by 17 kDa were purified (Fig. 2A), and they had the same N-terminal amino acid sequence. Because there are two potential N- and five predicted

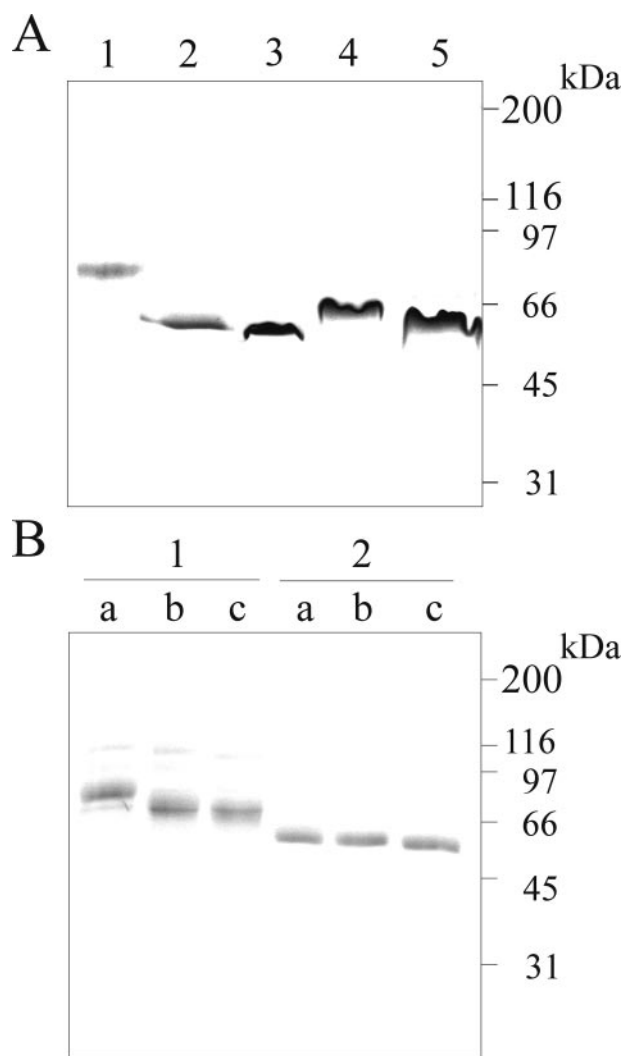


**FIGURE 2. SDS-PAGE of recombinant fibulins.** *A*, purified fibulins. The lanes were loaded with mouse fibulin-3, high molecular weight (1), mouse fibulin-3, low molecular weight (2), mouse fibulin-4 (3), mouse fibulin-5 (4), and human fibulin-5 (5) after reduction with dithiothreitol. *B*, deglycosylation of mouse fibulin-3. The lanes were loaded with fibulin-3, high molecular weight (1) and fibulin-3, low molecular weight (2) after incubation without enzymes (*a*) with neuraminidase and *O*-glycosidase (*b*) and neuraminidase, *O*-glycosidase and *N*-glycosidase F (*c*) under non-denaturing conditions. Electrophoresis was performed under reducing condition. Molecular mass markers are shown on the right.

*O*-glycosylation sites in mouse fibulin-3, the possibility that these two forms resulted from different *N*- or *O*-glycosylations was assessed by treatment with sialidase, *O*-glycosidase, and *N*-glycosidase F (Fig. 2*B*). Digestion with sialidase and *O*-glycosidase but not *N*-glycosidase decreased the size of the 80 kDa fibulin-3, whereas these enzymes had little effect on the size of the 63-kDa form. The data indicated that the size difference of the two forms was attributed at least in part to *O*-glycosylation.

***O*-Glycan Profiles and Glycosylation Sites on Mouse Recombinant Fibulin-3**—The *O*-linked glycans on the 80-kDa mouse fibulin-3 were liberated by reductive  $\beta$ -elimination and analyzed as methylated alditols by MALDI- and ESI-MS. The former revealed a series of dominant molecular ion signals  $M+Na$  at  $m/z$  895 (NeuAc<sub>1</sub>Hex<sub>1</sub>HexNAc<sub>1</sub>), 1140 (NeuAc<sub>1</sub>Hex<sub>1</sub>HexNAc<sub>2</sub>), 1256 (NeuAc<sub>2</sub>Hex<sub>1</sub>HexNAc<sub>1</sub>), 1344 (NeuAc<sub>1</sub>Hex<sub>2</sub>HexNAc<sub>2</sub>), and 1705 (NeuAc<sub>2</sub>Hex<sub>2</sub>HexNAc<sub>2</sub>). Only minor signals were detected at  $m/z$

**TABLE 1**  
***O*-Glycan profiles of fibulin-3 expressed in EBNA-293 cells**

Oligosaccharide structure	Average mass of molecular ions [ $M+Na$ ]
	<i>m/z</i>
NeuAc $\alpha$ 2-6 Gal $\beta$ 1-3 GalNAc	895
NeuAc $\alpha$ 2-3Gal $\beta$ 1-3GalNAc GlcNAc $\beta$ 1-6 GalNAc	895
NeuAc $\alpha$ 2-3Gal $\beta$ 1-3 NeuAc $\alpha$ 2-6 GalNAc	1140
NeuAc $\alpha$ 2-3Gal $\beta$ 1-3 GalNAc	1256
[NeuAc $\alpha$ 2-3]Gal $\beta$ 1-4GlcNAc $\beta$ 1-6 GalNAc	1344
[NeuAc $\alpha$ 2-3]Gal $\beta$ 1-3 NeuAc $\alpha$ 2-3Gal $\beta$ 1-4GlcNAc $\beta$ 1-6 GalNAc	1705

983 (Hex<sub>2</sub>HexNAc<sub>2</sub>) and 1793 (NeuAc<sub>1</sub>Hex<sub>3</sub>HexNAc<sub>3</sub>). The structures of the glycans were confirmed by sequence analysis performed on the ESI(Qtof) instrument in the MS/MS mode (Table 1). The ion at  $m/z$  895 was revealed as a mixture of two isobaric trisaccharides NeuAc-Hex-HexNAc-ol ( $Z_1$  ion at  $m/z$  298) and Hex-(NeuAc)-HexNAc-ol ( $Z_{1\alpha}$  ion at  $m/z$  659). The dominant structures were identified as the disialylated core1 tetrasaccharide NeuAc-Hex-(NeuAc)-HexNAc-ol and the disialylated core2 hexasaccharide NeuAc-Hex-HexNAc-(NeuAc-Hex)-HexNAc-ol.

According to the bioinformatic prediction tool for mucin-type *O*-glycosylation (NetOGlyc 3.1), five sites within the N-terminal domains of the protein should be *O*-glycosylated (Thr-88, Thr-98, Thr-99, Thr-101, and Thr-109). Four of the predicted sites (Thr-88, Thr-98, Thr-99, and Thr-101) could be excluded by mass spectrometric analysis as carrying glycans, because they were found in different approaches in non-glycosylated peptides. Peptides containing the position Thr-109 were not found in any of the analyses, neither as glycopeptides nor as non-glycosylated peptides. This finding could be interpreted as a hint to a modification of peptide p106–134 (dotted line in Fig. 3). Nearly the entire protein was covered by non-glycosylated peptide fragments (gray lines in Fig. 3), including p23–105, p135–156, p186–194, p208–227, p294–312, p316–339, p349–358, p363–376, and p388–477. Peptides or amino acid positions not covered in any of the mass spectrometric approaches were p106–134, p157–207 (except p186–194), p228–315 (except p294–312), p340–348, p359–362, p377–387, and p478–493 (Fig. 3). Potential *O*-glycosylation sites could be the C-terminal positions Thr-485 and Ser-492, which were not predicted, but had quite high G-scores in NetOGlyc 3.1 and were not found as peptides in any of the mass spectrometric analyses (dotted line in Fig. 3).

**Structural Characterization of Fibulins**—Electron microscopic examination of recombinant fibulin-3, -4, and -5 after rotary shadowing revealed short rods of ~20-nm length with a globular domain at one end (Fig. 4). The globular domain of fibulin-4 appeared smaller than that of fibulins-3 and -5. This observation, in conjunction with the primary structures of the fibulins (Fig. 1), suggests that the globular domains represent the N-terminal-modified cbEGF modules.

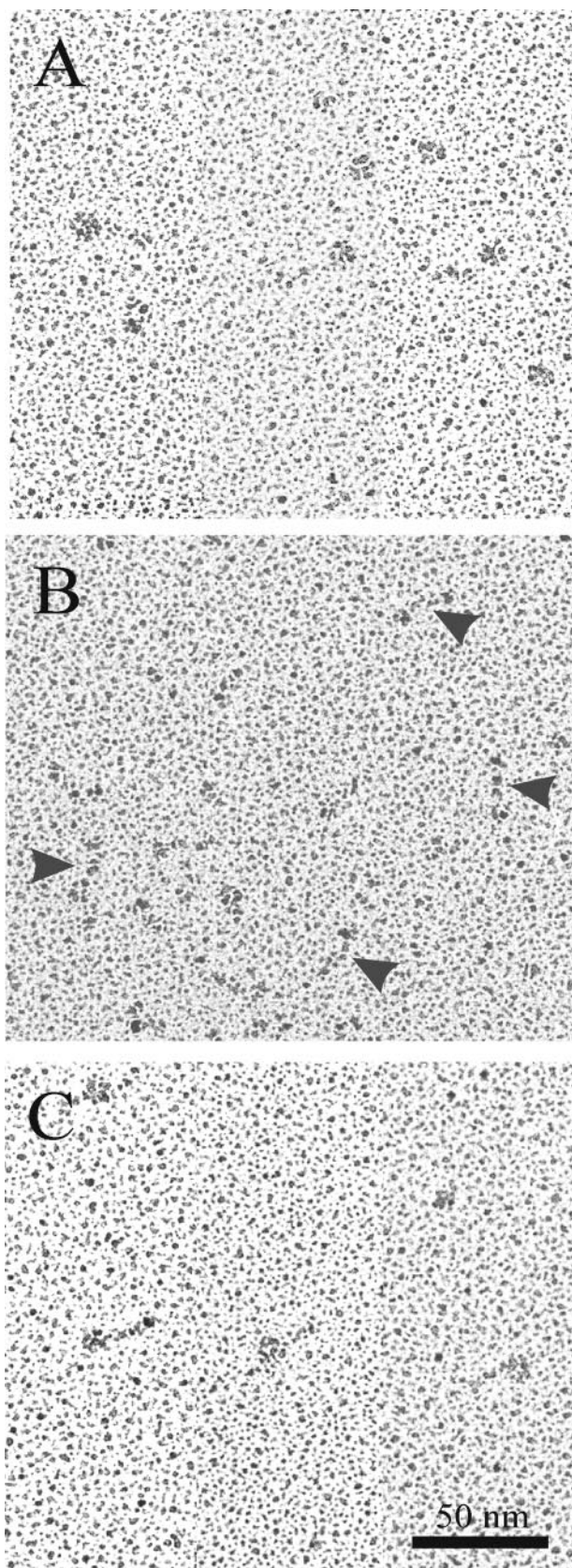


FIGURE 3. Rotary shadowing electron microscopy of recombinant fibulin-3 (A), fibulin-4 (B), and fibulin-5 (C). Arrowheads indicate typical views of fibulin-4. Bar represents 50 nm.

```

1      MLQTLFLTML TLALVKSQYT EETITYTQCT DGYEWDPIRQ QCKDIDECDI
51      VPDACKGGMK CVNHYGGYLC LPKTAQIVN NEHPQQETPA AEASSGA TTG
101     TVAARSMAIS GVVPGGGFMA SATAVAGPEV QTGRNNFVIR RNPADPQRIP
151     SNPSHRIQCA AGYEQEHNV CQDIDECTSG THNCRTDQVC INLRGSFTCQ
201     CLPGYQKRGE QCVDIDECTV PPYCHQRCVN TPGSFYCQCS PGFQLAANNY
251     TCVDINECDA SNQCAQQCYN ILGSFICQCN QGYELSSDRL NCEDIDECRT
301     SSYLCQYQCV NEPGKFSCMC PQGYEVVRSR TCQDINECET TNECREDEMC
351     WNYHGGFRCY PRNPCQDHYV LTSENRCVCP VSNTMCRELP QSIIVKYMSI
401     RSDRSVPSDI FQIQATMIYA NTINTFRIKS GNENGEFYLR QTSPVSAMLL
451     LVKSLSGPRE YIVDLEMLTV SSGTFRTRSS VLRL IIIVGP FSF
    
```

FIGURE 4. Glycosylation sites on recombinant mouse fibulin-3. Thr-88, Thr-98, Thr-99, Thr-101, and Thr-109 predicted to be O-glycosylated are in bold. Gray lines mark non-glycosylated peptides identified by mass spectrometry, and dotted lines indicate peptides that are likely to be O-glycosylated (p106–134 and p478–493).

In addition to the monomers shown in Fig. 4, some aggregates were also detected by electron microscopy. This is consistent with previous studies of recombinant human fibulin-4 by analytical centrifugation, showing considerable amounts of aggregates in addition to monomers (17). To determine whether oligomers exist under physiological conditions, recombinant mouse fibulin-4 and -5 were analyzed by molecular sieve chromatography with simultaneous detection of laser light scattering, refractive index, and absorbance at 230 nm. The two fibulins eluted as monomers, and the calculated molecular masses of fibulin-4 and -5 were 55 and 51 kDa, respectively. Further analysis of the eluted protein fractions using equilibrium ultracentrifugation confirmed the data obtained with laser light scattering. These results indicated that recombinant mouse fibulin-4 and -5 do not form oligomers under physiological conditions.

**Binding to Extracellular Matrix Proteins**—Solid-phase binding assays were performed with all five fibulins as soluble ligands in binding buffer containing 2 mM CaCl<sub>2</sub>. The binding to tropoelastin was characteristic for all five fibulins, extending the previous observations on fibulin-1 and -2 (45), fibulin-4 (23), and fibulin-5 (21, 22). The concentrations required for half-maximal binding were calculated to be 1–2 nM for fibulin-2 and fibulin-5, 8 nM for fibulin-4, and 42 nM for fibulin-1C (Fig. 5D). Binding of fibulin-3 to tropoelastin was rather weak, because the plateau level of binding was not reached even at a concentration of 1 μM. No binding of any fibulin to MAGP-1 and MAGP-2, two microfibril-associated proteins, was observed. In contrast to fibulin-1 and -2, Fibulin-3, -4, and -5 did not show any binding to fibronectin, vitronectin, laminin-1, perlecan, and nidogen-1 (Fig. 5C and data not shown). However, comparable interactions with collagen IV and nidogen-2

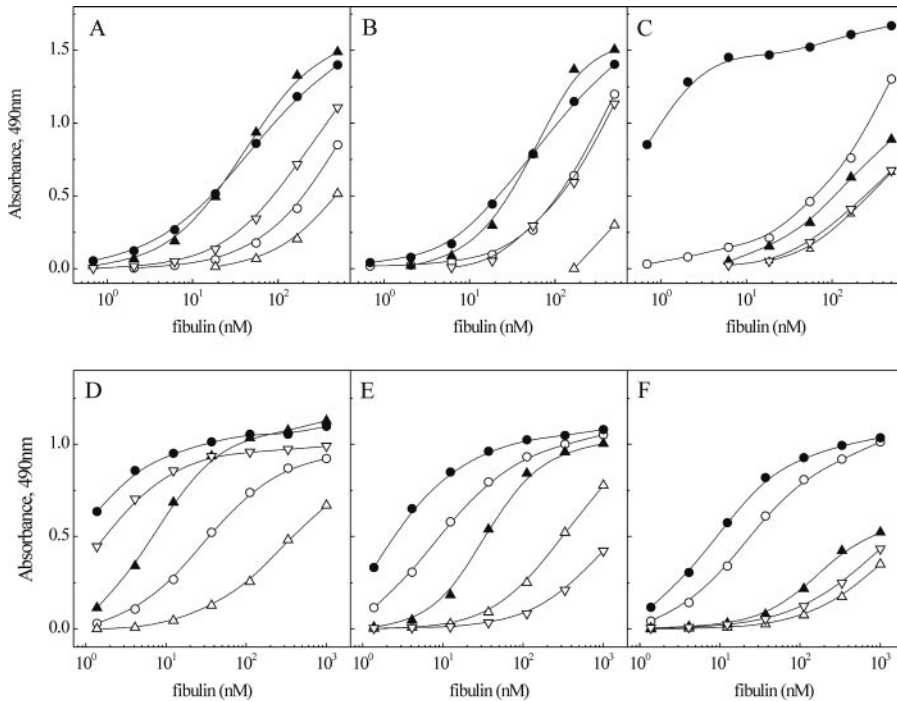


FIGURE 5. Binding of mouse fibulins to immobilized mouse collagen IV(A), mouse nidogen-2 (B), fibronectin (C), tropoelastin (D), endostatin domain of mouse collagen XV (E), and that of mouse collagen XVIII (F). Soluble ligands were fibulin-1C (○), fibulin-2 (●), fibulin-3 (△), fibulin-4 (▲), and fibulin-5 (▽).

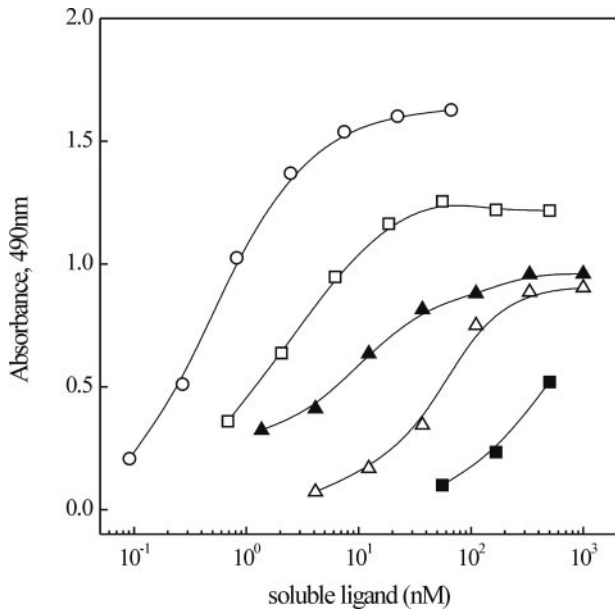


FIGURE 6. Solid-phase binding assay to immobilized  $\alpha$ V $\beta$ 3 integrin. Soluble ligands used were vitronectin (○), mouse fibulin-2 (□), human fibulin-2 (■), human fibulin-5 (△), and reduced and alkylated human fibulin-5 (▲).

were found for fibulin-4 and -2, having a half-maximal binding at 30–50 nM (Fig. 5, A and B). Fibulin-1 and -2 bind to endostatins, the C-terminal fragments released from collagens XV and XVIII (32). Fibulin-4 also exhibited a moderate binding to collagen XV-derived endostatin and a weak interaction with collagen XVIII endostatin. Weaker bindings to endostatins were observed for fibulin-3 and -5, which did not reach plateau levels at 1  $\mu$ M (Fig. 5, E and F).

**Cell Adhesion and Integrin Binding**—The cell adhesive properties of all fibulins were examined in parallel using various

established cell lines and human umbilical cord endothelial cells. Only mouse fibulin-2 was able to promote adhesion by several cell lines, as demonstrated previously (46) (data not shown). To test whether the RGD site in fibulin-5 had binding activity, purified  $\alpha$ V $\beta$ 3 integrin was used as the immobilized ligand (Fig. 6). The  $\alpha$ V $\beta$ 3 integrin showed a strong binding to vitronectin (half-maximal at 0.35 nM), moderate binding to mouse fibulin-2 (1.5 nM) as described before (46), but much weaker binding to human fibulin-5 (14 nM) and mouse fibulin-5 (data not shown). The binding activity of human fibulin-5 was increased after reduction and alkylation, indicating that the treatment unmasked the RGD site. However, the integrin binding activity of the unmasked fibulin-5 was still  $\sim$ 10-fold lower compared with vitronectin.

**Immunochemical Properties**—Rabbit antisera were raised against mouse fibulin-3, -4, and -5 and purified by affinity chromatography. The purified antibodies were highly specific with negligible cross-reactions among different fibulins (Fig. 7). This suggests that the antibodies should be able to distinguish the fibulin isoforms in complex biological specimens.

**Characterization of Fibulins in Fibroblast Cultures and Tissues**—The distribution of fibulin-3, -4, and -5 between the culture medium and three cell layer extracts of embryonic mouse fibroblasts was analyzed by immunoblotting (Fig. 8). The detergent extract is assumed to contain mainly the intracellular pool, whereas the EDTA and urea extracts consist of proteins that are deposited in the extracellular matrix. Fibulin-3 was found in low amounts in the culture medium and not in the three cell extracts in the amounts used for the analysis (data not shown). Fibulin-4 was detected in the culture medium and in all three cell extracts, whereas fibulin-5 was found in the three cell extracts but was not detected in 10  $\mu$ l of the conditioned medium. Higher amounts of fibulin-4 and -5 were observed in EDTA extracts as compared with the urea extracts, indicating a calcium requirement for their matrix association.

Tissues from adult mice were sequentially extracted with EDTA/TBS (EDTA extract) and the same buffer containing 1%Nonidet P-40, 0.5% sodium deoxycholate, 0.1% SDS (detergent extract) or 6 M guanidine hydrochloride (guanidine extract). These extracts were analyzed by immunoblotting (Fig. 9). For fibulin-3 and -4, almost all of the proteins from the aorta and >90% of lung proteins were extracted by the EDTA/TBS. The remaining 10% of these fibulins in the lung tissue were released by extraction with detergent. On the other hand, although the majority of fibulin-5 was detected in the first two extracts from both aorta and lung tissues,  $\sim$ 15–20% of the pro-

## A Comparative Analysis of the Fibulin Protein Family

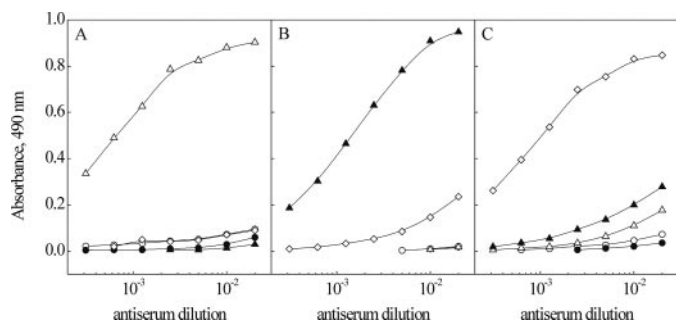


FIGURE 7. Enzyme-linked immunosorbent assay titration of rabbit antisera against mouse fibulin-3 (A), fibulin-4 (B), and fibulin-5 (C). Antigens used were fibulin-1C (○), fibulin-2 (●), fibulin-3 (△), fibulin-4 (▲), and fibulin-5 (◇).

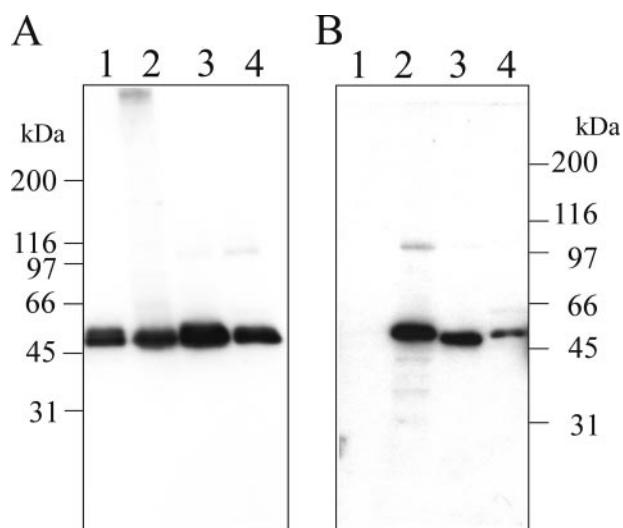


FIGURE 8. Immunoblot analysis of fibulin-4 (A) and fibulin-5 (B) in various mouse fibroblast compartments. Samples used were serum-free culture medium (1) and successive cell extracts obtained with detergent (2), EDTA (3), and 6 M urea (4). 10  $\mu$ l of each sample was separated under non-reducing conditions. Positions of molecular weight markers are indicated.

tein was present in the guanidine extract. These data may reflect the abundance of fibulin-5 in these tissues, its tight incorporation into the matrix, or both. It is noteworthy that, in addition to the major fibulin-3 band, a slower and a faster migrating protein were found in EDTA extracts, and the slower band was slightly faster than that of the *O*-glycosylated recombinant protein. The observation suggested the presence of differently glycosylated fibulin-3 in the tissues.

The tissue contents of fibulins in EDTA and detergent extracts were quantified by specific radioimmunoassays. The half-maximal inhibition was achieved at 18 ng/ml for fibulin-3, 10 ng/ml for fibulin-4, and 30 ng/ml for fibulin-5. These data were presented as the sum of the amounts in both extracts (Table 2). From most of the tissues, 60–90% of fibulins were extracted with EDTA/TBS. Radioimmunoassay analysis revealed that, in almost all tissues examined, fibulins-1 and -5 were substantially more abundant than the other three fibulins. All of the five fibulins were prevalent in tissues enriched in elastic fibers, including aorta, lung, and esophagus. However, their tissue distributions were not identical. For instance, fibulin-5 was detected at higher concentrations in aorta and lung, and fibulin-1 in esophagus and placenta.

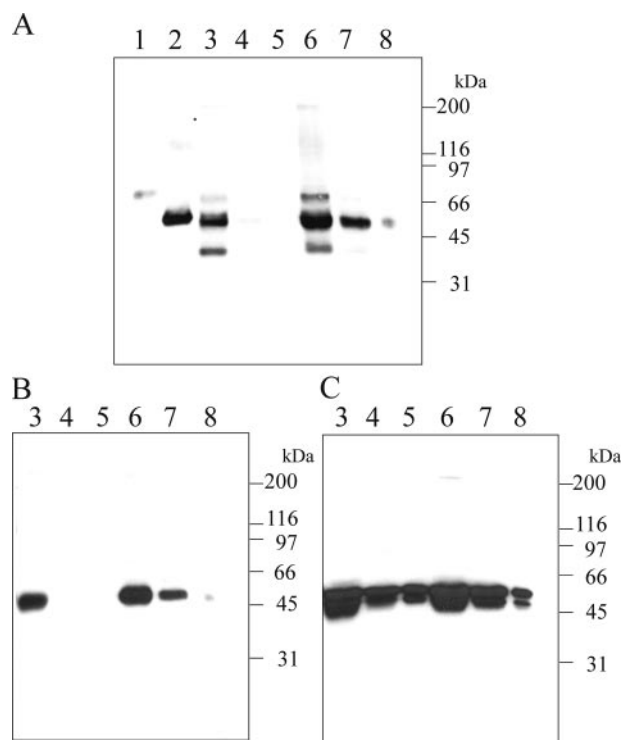


FIGURE 9. Detection of fibulin-3 (A), fibulin-4 (B), and fibulin-5 (C) in extracts from mouse aorta and lung. The extractions were performed as described under "Experimental Procedures." Comparable volumes of EDTA extract (3 and 6), detergent extract (4 and 7), and guanidine extract (5 and 8) were loaded and separated on 5–20% gradient gels under non-reducing conditions. Samples in lanes 3–5 were from mouse aorta, and those in lanes 6–8 were from mouse lung. Lanes 1 and 2 were loaded with 3 ng of recombinant fibulin-3, high molecular weight, and fibulin-3, low molecular weight, respectively. Positions of molecular mass markers are shown on the right.

TABLE 2  
Contents of fibulins in extracts of adult mouse tissues determined by radioimmunoassay/inhibition assays

Tissues were extracted by EDTA-containing buffer followed by detergent, and the sums in both extracts were calculated as picomoles obtained from 1 g of wet tissue.

Tissues	Fibulin-1	Fibulin-2	Fibulin-3	Fibulin-4	Fibulin-5
	<i>pmol</i>				
Aorta	173	56	95	78	963
Skin	73	20	31	11	21
Lung	180	35	304	17	878
Esophagus	712	30	104	32	332
Stomach	214	26	89	14	66
Intestine	178	27	78	23	160
Kidney	117	21	30	12	49
Heart	130	25	8	6	71
Skeletal muscle	80	21	68	30	104
Placenta	337	26	32	34	96
Brain	71	27	<2	42	49
Testis	97	33	66	56	300
Thymus	70	17	11	7	35
Spleen	172	37	58	55	319

**Immunolocalization of Fibulins**—Affinity-purified antibodies against the fibulins were used to immunostain cryosections of mouse embryos at 14 and 15 days of development. All five fibulins were found in the perichondrium of the developing bone in the E15 embryo (Fig. 10, A–E). Fibulin-1 was diffusely and intensely expressed in the basement membrane of tissues surrounding the bone, whereas the expression of the other four fibulins in these regions was more restricted to the basement membrane. In the E14 embryonic lung (Fig. 10, F–J), fibulin-1 was distinctly localized in the basement membrane of all air-

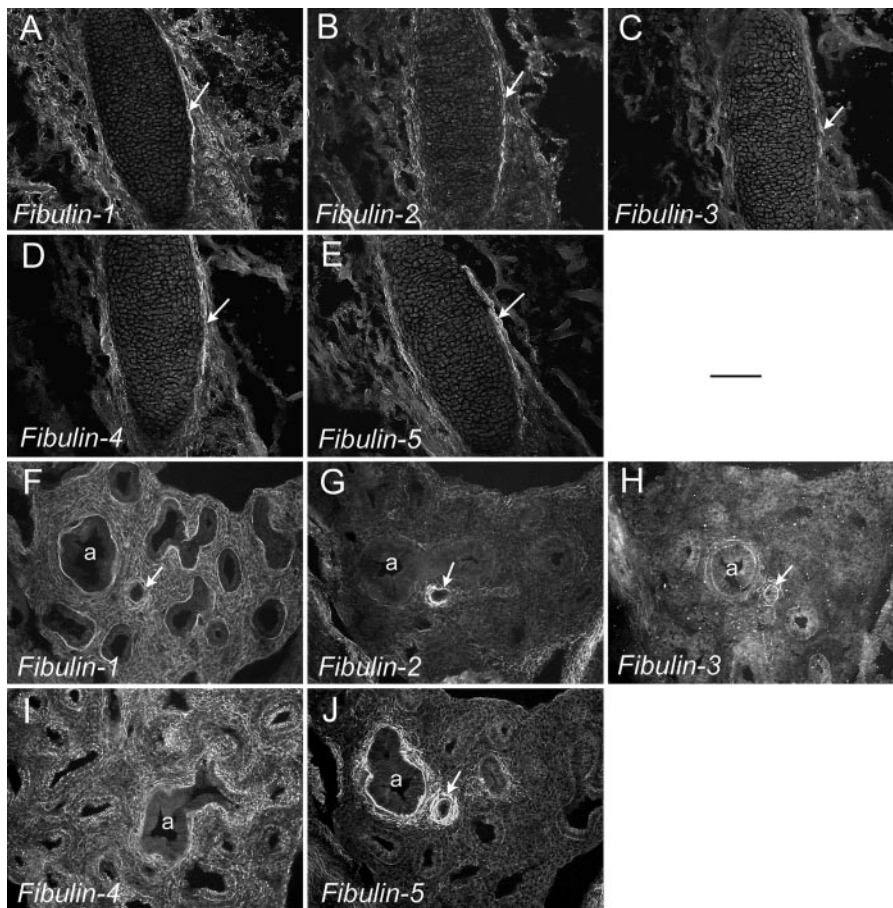


FIGURE 10. Localization of fibulin proteins in mouse tissues. Cryosections of E14 and E15 mouse embryos were immunostained with affinity-purified antibodies, and positive signals were revealed with Cy3-labeled secondary antibody. A–E, sections of a developing bone in the E15 mouse embryos. Arrows depict the perichondrial region. F–J, embryonic lung at E14. Arrows depict the blood vessels of the developing lung, and “a” marks the large airway. Bar = magnification 100  $\mu$ m.

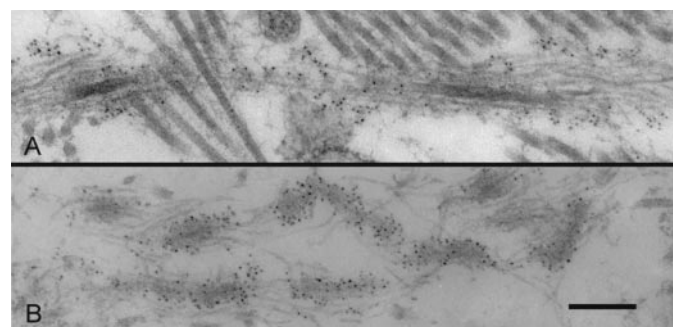


FIGURE 11. Ultrastructural localization of fibulin-4 and -5 in newborn mouse perichondrium. In A, fibulin-4-directed immunogold labeled the microfibrils surrounding elastin cores. In contrast, fibulin-5-directed immunogold preferentially labeled the interface between elastin cores and microfibrils (B). Bar = 100 nm.

ways and blood vessels and strongly and diffusely expressed throughout the lung parenchyma. Fibulin-2 expression was restricted to blood vessels and was totally absent from all airways and lung parenchyma. Fibulin-3 was mainly localized in the blood vessel wall and basement membrane of the large but not distal airways. Fibulin-4, like fibulin-1, was diffusely and strongly expressed in the lung parenchyma, but the expression in the basement membrane of the large airways was not as distinct as fibulin-1. Fibulin-5 is prominently expressed in the

blood vessel wall and in the basement membrane and parabronchial area of the large airway. However, it is weakly present in the lung parenchyma and distal airways.

Mouse newborn perichondrium was used to localize fibulin-4 and -5 at the ultrastructural level using *en bloc* diffusion method. The labeling of fibulin-4 was found in the microfibrils surrounding elastin cores (Fig. 11A), and fibulin-5 was detected at the interface between elastin cores and microfibrils (Fig. 11B).

## DISCUSSION

Members of the second subgroup of the fibulin family, fibulin-3, -4, and -5, have strikingly similar modular structure (Fig. 1), but their N-terminal-modified cbEGF modules differ in size. There are, 88, 28, and 44 amino acids inserted between the fourth and fifth cysteines of the modified cbEGF modules in fibulin-3, -4, and -5, respectively. Their sequence identities are ~50%, and the score is slightly lower (42.5%) between fibulin-3 and -5. Electron microscopy of the recombinant fibulin-3, -4, and -5 demonstrated a short rod structure with a globule at one end as expected for molecules with tandem EGF-like

modules (Fig. 4). Our analyses indicate that these three fibulins mainly exist as monomers under physiological conditions. By contrast, fibulin-2 forms dimers through covalent bonding, and fibulin-1 tends to self-associate into aggregates (31, 47, 48). The molecular masses calculated from the primary sequences are 53 kDa for fibulin-3, 46.8 kDa for fibulin-4, 47.7 kDa for mouse fibulin-5, and 48.9 kDa for human fibulin-5. Each fibulin has two potential N-glycosylation sites. Additionally, five O-glycosylation sites are predicted for fibulin-3, none for fibulin-4, three for mouse fibulin-5, and one for human fibulin-5. The molecular masses of the secreted recombinant proteins determined by SDS-electrophoresis (Fig. 2) are significantly larger than the predicted sizes, suggesting that these three fibulins are likely to have full substitutions with typical N-glycosides and probably also have O-glycosylation. EGF-like repeats and thrombospondin type 1 repeats are known to be O-fucosylated in several proteins, and a significant role for O-fucosylation of EGF repeats in Notch-ligand interaction has been reported (49–51). However, the consensus sequence proposed for O-fucosylation (51) is not present in all fibulins.

The isolation and characterization of the 80- and 63-kDa recombinant fibulin-3 proteins provides the first evidence for the presence of fibulin-3 isoforms that differ in O-glycosylation. Analysis of the O-glycosides liberated from 80-kDa fibulin-3 by

## A Comparative Analysis of the Fibulin Protein Family

mass spectrometry revealed an *O*-glycan profile similar to those of fusion proteins MUC1 and bone sialoprotein previously analyzed (37, 52). Because these fusion proteins were also expressed in the same 293 cell line as the recombinant fibulins, the results indicate that biosynthesis of *O*-glycan structures is less dependent on the protein scaffold but more determined by the cell-specific repertoire of glycosyltransferases. The dominance of sialylated core2 glycans can explain the only partial reduction in size of fibulin-3 after *O*-glycosidase treatment (Fig. 2B), because this enzyme cleaves specifically the core1 disaccharide. The mass difference between the two forms of fibulin-3 found by SDS-PAGE cannot be explained by the mass of glycans alone, but this is often the case for glycans containing sialic acids. Five different splice variants that differ in N-terminal sequences have previously been described for human fibulin-3, and only the largest and smallest variant are expressed in substantial amounts at the protein level (13). The 80- and 63-kDa forms of mouse fibulin-3 have the same N-terminal sequence and therefore unlikely to be the splice variants described in humans. Significantly, a fibulin-3 band with a size similar to the 80 kDa form could also be detected in mouse tissues (Fig. 9A). In addition, immunoblotting identified a faster migrating fibulin-3 band in tissues, which may correspond to the smallest splice variant or a proteolytic fragment. Whether fibulin-3 functions are modulated by the *O*-glycosylation, alternative splicing, or proteolytic processing awaits further investigation.

Homotypic and heterotypic interactions, including those with cellular receptors, are involved in matrix assembly and modulation of cellular phenotypes. Our studies demonstrate that the second subgroup of fibulins have more restricted binding repertoires than the first subgroup in that they do not interact with fibronectin and most basement membrane proteins examined. Fibulin-4 displays a somewhat broader binding spectrum than fibulin-3 and -5, because it is capable of interacting with collagen IV, nidogen-2, and collagen XV-derived endostatin in a manner similar to fibulin-2.

Tropoelastin is a common ligand for all five fibulins, and the binding strengths range from strong for fibulin-2 and -5, moderate for fibulin-1 and -4, to weak for fibulin-3. Immunohistochemical analyses corroborate these findings, showing that all five fibulins are localized in tissues rich in elastic fibers, such as lungs, perichondrium, and blood vessels. The results suggest that all fibulins may contribute to elastic fiber assembly or maintenance. To date, only fibulin-4 and -5 have been found to be essential for elastic fiber assembly (21–23). Absence of fibulin-1 or fibulin-2 in mice does not have apparent effects on elastic fiber homeostasis (53).<sup>5</sup> The lack of correlation between the strengths of tropoelastin binding *in vitro* and the elastic fiber phenotypes *in vivo* may be explained by functional compensation among the fibulins.

We show here by immunoelectron microscopy that fibulin-5 is present at the interface between elastin cores and microfibrils where fibulin-2 was previously localized (6). On the other hand, fibulin-4 labeling is preferentially found in the microfibrils sur-

rounding the elastin cores. Recently, both fibulin-4 and -5 have been shown to interact with fibrillin-1, the major constituent of microfibrils associated with elastic fibers (54, 55). Thus, these two fibulins likely serve as connecting proteins between elastin and fibrillin microfibrils, thereby playing essential roles in elastic fiber assembly and/or homeostasis. It is noteworthy that even though paucity and fragmentation of elastic fibers are similarly observed in mice lacking either fibulin-4 or fibulin-5, the fibulin-4 null mice die within 2 days after birth, whereas the fibulin-5 mice can survive until adulthood (21–23). The stark difference in phenotypic severity of the two mouse mutants implies that fibulin-4 may perform more critical functions than fibulin-5 during elastic fiber formation, or fibulin-4 has other additional roles. The broader binding repertoires of fibulin-4 compared with fibulin-5 is consistent with the latter possibility.

Apart from the relatively weak binding to tropoelastin, fibulin-3 displays little interaction with all ligands tested in this study. We did not detect any apparent difference in the binding properties of the two forms of fibulin-3 *in vitro* (data not shown). As with all other fibulins, fibulin-3 is present in blood vessels of different sizes. Like fibulin-5, fibulin-3 is capable of inhibiting vessel development and angiogenesis both *in vitro* and *in vivo* (56). Moreover, fibulin-3 is expressed in cartilage and bone structures during development and may play a role in the skeletal system (57). Whether fibulin-3 contributes to the structural integrity of elastic tissues has yet to be determined by genetic approaches. Fibulin-3 has previously been shown to be a strong interacting protein for TIMP-3, a tissue inhibitor of metalloproteinases. The biological significance of this interaction is highlighted by the observations that both TIMP-3 and fibulin-3 are associated with genetic macular degenerative disorders (15, 59, 60).

Mouse fibulin-2 has previously been shown to be cell adhesive and to interact with  $\alpha$ 1b $\beta$ 3 and  $\alpha$ V $\beta$ 3 integrins but not with  $\alpha$ 5 $\beta$ 1 integrin, and these interactions can be inhibited by RGD peptides (46). Mouse fibulin-2 contains a single RGD sequence at the N-terminal domain, and this sequence is RSS in human fibulin-2 (4, 61). Mouse and human fibulin-5 also contain an RGD sequence in the N-terminal-modified cbEGF module and have been shown to bind to  $\alpha$ V $\beta$ 3,  $\alpha$ V $\beta$ 5, and  $\alpha$ 9 $\beta$ 1 integrins (21). In the present study, we have analyzed the cell adhesive activity of all fibulins using several established cell lines previously shown to adhere in an RGD-dependent fashion. We confirmed that mouse fibulin-2 is a cell adhesive substrate, but none of the other fibulins, including fibulin-5, showed binding to all cell lines tested. These observations are at variance with the published data on fibulin-5 (21). Therefore we further performed binding analysis of fibulin-5 with purified  $\alpha$ V $\beta$ 3 integrin. Fibulin-5 showed only marginal binding, and denaturation of the protein increased the binding. These data suggest that the RGD site in fibulin-5 may not be fully exposed as shown for the mouse laminin P1 fragment (62) and mouse perlecan domain III-2 (63). We tried to model the modified cbEGF module containing the RGD site based on the structural data on the fibrillin cbEGF-like repeats (64). If the extra 44 amino acids were not inserted between the fourth and fifth cysteines in this cbEGF-like module, the RGD site would be accessible. However, currently we have no data on how the

<sup>5</sup> M. L. Chu, unpublished observation.

RGD residues are organized in the structure of the modified cbEGF module with the extra amino acids inserted. Structural analysis of the modified cbEGF module at the atomic level, such as shown for a masked RGD in thrombin, is required (58, 65).

In summary, we have compared the properties of all members of the fibulin family in parallel. We showed that each of the five fibulins displays distinct binding repertoires and tissue distribution. However, there are substantial overlaps in these characteristics among fibulins, and the similarities in the properties are higher among members within the same subgroups than those between subgroups. For instance, members in the first subgroup interact with both elastic fiber and basement membrane components, whereas those in the second subgroup bind primarily to elastic fiber components. All fibulins are expressed in elastic tissues, but their spatial localizations within tissues are distinct and also overlapping. Our studies suggest unique and redundant functions shared by these structurally related proteins and imply the existence of compensation mechanisms among the family members.

*Acknowledgments*—We are grateful for the excellent technical assistance of Vera van Delden, Christa Wendt, Mischa Reiter, Hanna Wiedemann, and Dorothea Jahn. We thank Dr. Karlheinz Mann for sequence analysis, Dr. Manuel Than for modeling of modified cbEGF module of fibulin-5, and Dr. Lynn Y. Sakai for critical reading of the manuscript.

## REFERENCES

1. Argraves, W. S., Greene, L. M., Cooley, M. A., and Gallagher, W. M. (2003) *EMBO Rep.* **4**, 1127–1131
2. Timpl, R., Sasaki, T., Kostka, G., and Chu, M. L. (2003) *Nat. Rev. Mol. Cell Biol.* **4**, 479–489
3. Chu, M. L., and Tsuda, T. (2004) *Birth Defects Res. Part C. Embryo. Today* **72**, 25–36
4. Pan, T. C., Sasaki, T., Zhang, R. Z., Fassler, R., Timpl, R., and Chu, M. L. (1993) *J. Cell Biol.* **123**, 1269–1277
5. Roark, E. F., Keene, D. R., Haudenschild, C. C., Godyna, S., Little, C. D., and Argraves, W. S. (1995) *J. Histochem. Cytochem.* **43**, 401–411
6. Reinhardt, D. P., Sasaki, T., Dzamba, B. J., Keene, D. R., Chu, M. L., Gohring, W., Timpl, R., and Sakai, L. Y. (1996) *J. Biol. Chem.* **271**, 19489–19496
7. Zhang, H. Y., Timpl, R., Sasaki, T., Chu, M. L., and Ekblom, P. (1996) *Dev. Dyn.* **205**, 348–364
8. Argraves, W. S., Tran, H., Burgess, W. H., and Dickerson, K. (1990) *J. Cell Biol.* **111**, 3155–3164
9. Kluge, M., Mann, K., Dziadek, M., and Timpl, R. (1990) *Eur. J. Biochem.* **193**, 651–659
10. Spence, S. G., Argraves, W. S., Walters, L., Hungerford, J. E., and Little, C. D. (1992) *Dev. Biol.* **151**, 473–484
11. Tsuda, T., Wang, H., Timpl, R., and Chu, M. L. (2001) *Dev. Dyn.* **222**, 89–100
12. Zhang, H. Y., Chu, M. L., Pan, T. C., Sasaki, T., Timpl, R., and Ekblom, P. (1995) *Dev. Biol.* **167**, 18–26
13. Lecka-Czernik, B., Lumpkin, C. K. J., and Goldstein, S. (1995) *Mol. Cell Biol.* **15**, 120–128
14. Blackburn, J., Tarttelin, E. E., Gregory-Evans, C. Y., Moosajee, M., and Gregory-Evans, K. (2003) *Invest. Ophthalmol. Vis. Sci.* **44**, 4613–4621
15. Stone, E. M., Lotery, A. J., Munier, F. L., Heon, E., Piguat, B., Guymer, R. H., Vandenburgh, K., Cousin, P., Nishimura, D., Swiderski, R. E., Silvestri, G., Mackey, D. A., Hageman, G. S., Bird, A. C., Sheffield, V. C., and Schorderet, D. F. (1999) *Nat. Genet.* **22**, 199–202
16. Gallagher, W. M., Argentini, M., Sierra, V., Bracco, L., Debussche, L., and Conseiller, E. (1999) *Oncogene* **18**, 3608–3616
17. Giltay, R., Timpl, R., and Kostka, G. (1999) *Matrix Biol.* **18**, 469–480
18. Gallagher, W. M., Greene, L. M., Ryan, M. P., Sierra, V., Berger, A., Laurent-Puig, P., and Conseiller, E. (2001) *FEBS Lett.* **489**, 59–66
19. Kowal, R. C., Richardson, J. A., Miano, J. M., and Olson, E. N. (1999) *Circ. Res.* **84**, 1166–1176
20. Nakamura, T., Ruiz-Lozano, P., Lindner, V., Yabe, D., Taniwaki, M., Furukawa, Y., Kobuke, K., Tashiro, K., Lu, Z., Andon, N. L., Schaub, R., Matsumori, A., Sasayama, S., Chien, K. R., and Honjo, T. (1999) *J. Biol. Chem.* **274**, 22476–22483
21. Nakamura, T., Lozano, P. R., Ikeda, Y., Iwanaga, Y., Hinek, A., Minamisawa, S., Cheng, C. F., Kobuke, K., Dalton, N., Takada, Y., Tashiro, K., Ross, J. J., Honjo, T., and Chien, K. R. (2002) *Nature* **415**, 171–175
22. Yanagisawa, H., Davis, E. C., Starcher, B. C., Ouchi, T., Yanagisawa, M., Richardson, J. A., and Olson, E. N. (2002) *Nature* **415**, 168–171
23. McLaughlin, P. J., Chen, Q., Horiguchi, M., Starcher, B. C., Stanton, J. B., Broekelmann, T. J., Marmorstein, A. D., McKay, B., Mecham, R., Nakamura, T., and Marmorstein, L. Y. (2006) *Mol. Cell Biol.* **26**, 1700–1709
24. Loeys, B., Van Maldergem, L., Mortier, G., Coucke, P., Gerniers, S., Naeyaert, J. M., and De Paepe, A. (2002) *Hum. Mol. Genet.* **11**, 2113–2118
25. Markova, D., Zou, Y., Ringpfeil, F., Sasaki, T., Kostka, G., Timpl, R., Uitto, J., and Chu, M. L. (2003) *Am. J. Hum. Genet.* **72**, 998–1004
26. Huchtagowder, V., Sausgruber, N., Kim, K. H., Angle, B., Marmorstein, L. Y., and Urban, Z. (2006) *Am. J. Hum. Genet.* **78**, 1075–1080
27. Stone, E. M., Braun, T. A., Russell, S. R., Kuehn, M. H., Lotery, A. J., Moore, P. A., Eastman, C. G., Casavant, T. L., and Sheffield, V. C. (2004) *N. Engl. J. Med.* **351**, 346–353
28. Timpl, R., Paulsson, M., Dziadek, M., and Fujiwara, S. (1987) *Methods Enzymol.* **145**, 363–391
29. Fox, J. W., Mayer, U., Nischt, R., Aumailley, M., Reinhardt, D., Wiedemann, H., Mann, K., Timpl, R., Krieg, T., and Engel, J. (1991) *EMBO J.* **10**, 3137–3146
30. Salmivirta, K., Talts, J. F., Olsson, M., Sasaki, T., Timpl, R., and Ekblom, P. (2002) *Exp. Cell Res.* **279**, 188–201
31. Sasaki, T., Kostka, G., Gohring, W., Wiedemann, H., Mann, K., Chu, M. L., and Timpl, R. (1995) *J. Mol. Biol.* **245**, 241–250
32. Sasaki, T., Larsson, H., Tisi, D., Claesson-Welsh, L., Hohenester, E., and Timpl, R. (2000) *J. Mol. Biol.* **301**, 1179–1190
33. Yatohgo, T., Izumi, M., Kashiwagi, H., and Hayashi, M. (1988) *Cell Struct. Funct.* **13**, 281–292
34. Pfaff, M., Gohring, W., Brown, J. C., and Timpl, R. (1994) *Eur. J. Biochem.* **225**, 975–984
35. Kohfeldt, E., Maurer, P., Vannahme, C., and Timpl, R. (1997) *FEBS Lett.* **414**, 557–561
36. Engel, J. (1994) *Methods Enzymol.* **245**, 469–488
37. Schulz, B. L., Packer, N. H., and Karlsson, N. G. (2002) *Anal. Chem.* **74**, 6088–6097
38. Engelmann, K., Kinlough, C. L., Muller, S., Razawi, H., Baldus, S. E., Hughey, R. P., and Hanisch, F. G. (2005) *Glycobiology* **15**, 1111–1124
39. Aumailley, M., Wiedemann, H., Mann, K., and Timpl, R. (1989) *Eur. J. Biochem.* **184**, 241–248
40. Aumailley, M., Timpl, R., and Sonnenberg, A. (1990) *Exp. Cell Res.* **188**, 55–60
41. Timpl, R. (1982) *Methods Enzymol.* **82**, 472–498
42. Sasaki, T., Wiedemann, H., Matzner, M., Chu, M. L., and Timpl, R. (1996) *J. Cell Sci.* **109**, 2895–2904
43. Sakai, L. Y., and Keene, D. R. (1994) *Methods Enzymol.* **245**, 29–52
44. Mayer, U., Nischt, R., Poschl, E., Mann, K., Fukuda, K., Gerl, M., Yamada, Y., and Timpl, R. (1993) *EMBO J.* **12**, 1879–1885
45. Sasaki, T., Gohring, W., Miosge, N., Abrams, W. R., Rosenbloom, J., and Timpl, R. (1999) *FEBS Lett.* **460**, 280–284
46. Pfaff, M., Sasaki, T., Tangemann, K., Chu, M. L., and Timpl, R. (1995) *Exp. Cell Res.* **219**, 87–92
47. Balbona, K., Tran, H., Godyna, S., Ingham, K. C., Strickland, D. K., and Argraves, W. S. (1992) *J. Biol. Chem.* **267**, 20120–20125
48. Sasaki, T., Mann, K., Wiedemann, H., Gohring, W., Lustig, A., Engel, J., Chu, M. L., and Timpl, R. (1997) *EMBO J.* **16**, 3035–3043
49. Hofsteenge, J., Huwiler, K. G., Macek, B., Hess, D., Lawler, J., Mosher, D. F., and Peter-Katalinic, J. (2001) *J. Biol. Chem.* **276**, 6485–6498
50. Haines, N., and Irvine, K. D. (2003) *Nat. Rev. Mol. Cell Biol.* **4**, 786–797

## A Comparative Analysis of the Fibulin Protein Family

51. Harris, R. J., and Spellman, M. W. (1993) *Glycobiology* **3**, 219–224
52. Wuttke, M., Muller, S., Nitsche, D. P., Paulsson, M., Hanisch, F. G., and Maurer, P. (2001) *J. Biol. Chem.* **276**, 36839–36848
53. Kostka, G., Giltay, R., Bloch, W., Addicks, K., Timpl, R., Fassler, R., and Chu, M. L. (2001) *Mol. Cell. Biol.* **21**, 7025–7034
54. Freeman, L. J., Lomas, A., Hodson, N., Sherratt, M. J., Mellody, K. T., Weiss, A. S., Shuttleworth, C. A., and Kielty, C. M. (2005) *Biochem. J.* **388**, 1–5
55. El-Hallous, E., Sasaki, T., Hubmacher, D., Getie, M., Tiedemann, K., Brinckmann, J., Bätge, B., Davis, E. C., and Reinhardt, D. P. (2007) *J. Biol. Chem.* **282**, 8935–8946
56. Albig, A. R., Neil, J. R., and Schiemann, W. P. (2006) *Cancer Res.* **66**, 2621–2629
57. Ehlermann, J., Weber, S., Pfisterer, P., and Schorle, H. (2003) *Gene Expr. Patterns.* **3**, 441–447
58. Bode, W., Turk, D., and Karshikov, A. (1992) *Protein Sci.* **1**, 426–471
59. Weber, B. H., Vogt, G., Pruett, R. C., Stohr, H., and Felbor, U. (1994) *Nat. Genet.* **8**, 352–356
60. Klenotic, P. A., Munier, F. L., Marmorstein, L. Y., and Anand-Apte, B. (2004) *J. Biol. Chem.* **279**, 30469–30473
61. Zhang, R. Z., Pan, T. C., Zhang, Z. Y., Mattei, M. G., Timpl, R., and Chu, M. L. (1994) *Genomics* **22**, 425–430
62. Aumailley, M., Timpl, R., and Risau, W. (1991) *Exp. Cell Res.* **196**, 177–183
63. Schulze, B., Sasaki, T., Costell, M., Mann, K., and Timpl, R. (1996) *Matrix Biol.* **15**, 349–357
64. Downing, A. K., Knott, V., Werner, J. M., Cardy, C. M., Campbell, I. D., and Handford, P. A. (1996) *Cell* **85**, 597–605
65. Bar-Shavit, R., Maoz, M., Ginzburg, Y., and Vlodavsky, I. (1996) *J. Cell. Biochem.* **61**, 278–291